Journal of Hazardous Materials 443 (2023) 130119

Contents lists available at ScienceDirect

Journal of Hazardous Materials

journal homepage: www.elsevier.com/locate/jhazmat

Research Paper

Plant rhizosphere defense system respond differently to emerging polyfluoroalkyl substances F-53B and PFOS stress

Bianhe Lu [a,b], Jin Qian [a,b,*], Jing Hu [c], Yuanyuan Huang [d], Peifang Wang [a,b,*], Junwei Shen [a,b], Yuxuan He [a,b], Sijing Tang [a,b], Yin Liu [a,b], Yuhang Zhang [a,b]

[a] Key Laboratory of Integrated Regulation and Resource Development on Shallow Lakes, Ministry of Education, Hohai University, Nanjing 210098, People's Republic of China
[b] College of Environment, Hohai University, Nanjing 210098, People's Republic of China
[c] Geosystems Research Institute, Mississippi State University, MS 39759, USA
[d] CSIRO Oceans and Atmosphere, Aspendale 3195, Australia

HIGHLIGHTS

- Both PFASs affected the properties and microbial communities of the bulk soils.
- Different types and levels of PFAS resulted in different root exudates.
- Root exudates and PFAS together influenced the rhizosphere microbial community.
- F-53B leads to greater rhizosphere defense system response.
- The response of the rhizosphere defense system is plant-specific.

GRAPHICAL ABSTRACT

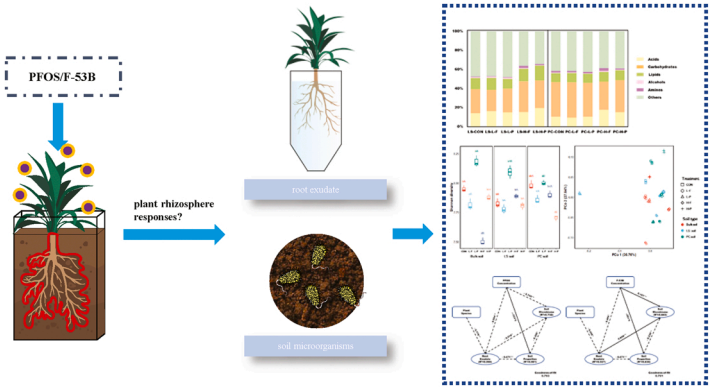

ARTICLE INFO

Dr. Karina S. B. Miglioranza

Keywords:
Perfluorooctanesulfonate
Chlorinated polyfluoroalkyl ether sulfonate
Microbial community
Root exudate
Partial least squares pathway model

ABSTRACT

Chlorinated polyfluoroalkyl ether sulfonate (F-53B) and perfluorooctanesulfonate (PFOS) are used and emitted as fog inhibitors in the chromium plating industry, and they are widely detected worldwide. To study the effects of F-53B and PFOS on the rhizosphere defense system, they were added at two levels (0.1 and 50 mg L^{-1}) to the soil where different plants (*Lythrum salicaria* and *Phragmites communis*) were grown. In bulk soils, high concentrations of F-53B/PFOS resulted in significant increases in soil pH, NH_4^+-N, and NO_3^--N (the effect of PFOS on NO_3^--N was not significant). Moreover, the extent of the effects of PFOS and F-53B on the physicochemical properties of bulk soils were different (e.g., PFOS caused an increase of NH_4^+-N by 8.94%−45.97% compared to 1.63%−25.20% for F-53B). Root exudates and PFASs together influenced the physicochemical properties of rhizosphere soils (e.g., TOC increased significantly in contaminated rhizosphere soils but did not change in non-bulk soils). Under the influence of F-53B/PFOS, the root exudates regulated by plants were changed and

* Corresponding authors at: Key Laboratory of Integrated Regulation and Resource Development on Shallow Lakes, Ministry of Education, Hohai University, Nanjing 210098, People's Republic of China.
E-mail addresses: hhuqj@hhu.edu.cn (J. Qian), pfwang2005@hhu.edu.cn (P. Wang).

https://doi.org/10.1016/j.jhazmat.2022.130119
Received 7 May 2022; Received in revised form 30 September 2022; Accepted 1 October 2022
Available online 4 October 2022

weakened the effect of F-53B/PFOS on microbial community of rhizosphere soil. The rhizosphere defense systems of different plants have both similarities and differences in response to different substances and concentrations.

1. Introduction

Perfluorooctanesulfonate (PFOS) has been commonly used in the manufacture of paper, textile and leather for nearly half a century (Qian et al., 2019). PFOS is considered a major health hazard due to its chemical stability, bioaccumulation properties, and toxicity to living organisms (Abdel-Gawad et al., 2016; Briels et al., 2018; Huang et al., 2015). The major manufacturer 3 M voluntarily phased out PFOS in 2000, which started a series of measures to restrict the production and use of the compound (Briels et al., 2018; Mao et al., 2018). In May 2009, PFOS and its salts were listed in Annex B of the Stockholm Convention on Persistent Organic Pollutants by the Fourth Meeting of the Parties (Stokke and Thommessen, 2013). However, due to the lack of readily available alternatives, the electroplating industry is one of the Convention exemptions for the production and use of PFOS (Stokke and Thommessen, 2013).

In China, a country with a well-developed electroplating industry, the chlorinated polyfluoroalkyl ether sulfonate (6: 2 Cl-PFESA, trade name F-53B) has started to be used as a fluorinated alternative for PFOS (Wang et al., 2013). Due to its low production cost and reduction in the use of PFOS, the demand for F-53B is seen to increase for the Chinese mist suppressant market (Ruan et al., 2015). Both PFOS and F-53B enter surrounding environments during production, use, and disposal, and have been detected in a variety of environmental media, including air, soil, aquatic systems and biological samples (Qian et al., 2019). The presence and potential hazards of F-53B in the environment have been overlooked for decades (Briels et al., 2018; Wang et al., 2013). Like PFOS, F-53B is environmentally persistent, indicating that F-53B can potentially be distributed and continuously accumulated globally (Briels et al., 2018; Gomis et al., 2015). And similar to PFOS (Nakayama et al., 2005), the concentration of F-53B in natural waters is up to mg L^{-1} level (Ti et al., 2018). Many existing studies have highlighted the developmental toxicity, immunotoxicity, genotoxicity and neurotoxicity of PFOS in individuals (Briels et al., 2018; Qian et al., 2019). However, there are relatively few studies on the environmental impact of F-53B. As the substitute of PFOS, F-53B differs from PFOS in terms of molecular structure and molecular energy (Fig. S1), which can lead to different physical and chemical properties. For instance, Deng et al. (2018) found that F-53B is more bioaccumulative than PFOS. Therefore, it can be inferred that the environmental effects of F-53B and PFOS are different.

The root-soil-microbe interaction mediated by root exudates constitutes an essential part of the defense strategy of plants in soil (Baetz and Martinoia, 2014; Doornbos et al., 2012; Hu et al., 2018; Siqueira et al., 1991). The rhizosphere defense system provides services for plants to adapt to pollution stress or nutrient deficiency (Baetz and Martinoia, 2014; Carvalhais et al., 2011; Hu et al., 2018; Huang et al., 2016). To the best of our knowledge, no study has yet compared the effects of F-53B and PFOS on the rhizosphere defense system in the soil. Riparian plants are often used in riparian ecological restoration and sewage treatment plants for advanced treatment (Hale et al., 2018; Soda et al., 2012), and are the type of plants having the most exposure to PFOS and F-53B (Gao et al., 2017; Lechner and Knapp, 2011; Qian et al., 2017). Evaluating the responses of riparian plant rhizosphere defense system to these two per- and polyfluoroalkyl substances (PFAS) can serve as a pilot study for comparing the environmental and ecological impacts of F-53B and PFOS.

In this study, an indoor microenvironmental study was conducted to characterize the root exudates and rhizosphere microbial communities of two typical riparian plants under the influence of different concentrations of F-53B and PFOS, in order to explore the differences in plant rhizosphere defense systems in response to F-53B and PFOS stresses.

2. Methods

2.1. Materials and reagents

F – 53B and PFOS were purchased from Shanghai Synica and Sigma-Aldrich Co., with purity of > 98%. Two dominant riparian plants in Taihu Lake Basin, eastern China, the perennial herb *Lythrum salicaria* (Ls, dicotyledonous) and the reed *Phragmites communis* (Pc, monocotyledonous), were selected in the study (Lu et al., 2020a). To avoid atypically high absorption rates which may be seen in young plants (Qian et al., 2019), healthy, homogeneous, lab-grown plants aged 3 months were used for the exposure experiment. After 7 days of filter paper germination, the plants were transferred to a half-strength Hoagland's solution (Qian et al., 2019) in an artificial climate chamber for two and a half months, and then transferred to the prepared soil in the experimental climate chamber for a further half month prior to rhizobox planting. The soil (pH 7.1) was obtained from the riparian of the Wangyu River in the Taihu Lake Basin of Wuxi City, Jiangsu Province, China (31°27'00"N, 120°29'02"E). According to FAO/WRB soil classification, the soil is Gleysol. And the soil consisted of 11.9% sand, 42.2% silt and 45.9% clay, with an organic matter content of 2.13%, and a total organic carbon of 14.57 g kg^{-1}, total nitrogen of 2.78 g kg^{-1}, available nitrogen of 486.74 mg kg^{-1}, total phosphorus of 0.35 g kg^{-1}, available phosphorus of 4.35 mg kg^{-1}, total potassium of 1.63 g kg^{-1}, available potassium of 98.71 mg kg^{-1}, cation exchange capacity of 18.36 meq 100 g^{-1} and electric conductivity of 0.42 dS m^{-1}. PFOS and F-53B were not detected in the collected soils (Detection limit: 0.49 ng g^{-1} dry weight and 1.12 ng g^{-1} dry weight, respectively). The soil was dried, ground and sieved (2 mm), then sterilized by autoclaving at 121 °C for 45 min over three consecutive days (Pan and Chu, 2016).

2.2. Experimental design

Plants were grown in rhizoboxes (interior: 3 cm × 30 cm × 40 cm, Fig. S2) with 3.5 ± 0.1 kg soils. There are 3 watering holes near the base of each rhizobox (Fig S2). A riparian microenvironment is created by hose-connecting the watering holes of the rhizobox and a plastic bucket (interior: 12 cm × 20 cm × 44 cm) filled with polyfluoroalkyl substance solution. The hoses took on the role of solution inflow and outflow from the rhizobox. The height of the solution in the plastic bucket was maintained at 25 cm. Forty-five riparian microenvironmental devices were randomly selected to subject to five treatments: (i) control: distilled water in the plastic bucket; (ii) low PFOS contamination: distilled water with 0.1 mg L^{-1} PFOS (low PFOS); (iii) high PFOS contamination: distilled water with 50 mg L^{-1} PFOS (high PFOS); (iv) low F-53B contamination: distilled water with 0.1 mg L^{-1} F-53B (low F-53B); and (v) high F-53B contamination: distilled water with 50 mg L^{-1} F-53B (high F-53B). The low concentration (0.1 mg L^{-1}) treatment group was used to simulate the concentration of contaminants in the current natural water, while the high concentration (50 mg L^{-1}) treatment group was used to simulate emergency events such as high accumulation of contaminants or contaminant spills. Six of the nine rhizoboxes under each treatment were randomly assigned for *P. communis* and *L. salicaria,* with 3 for each species. Each rhizobox was planted with one plant seedling. The remaining 3 rhizoboxes of each treatment without plant were for the bulk soil sampling. At the beginning of the experiment, 100 ml of half-strength Hoagland's solution was administered to each rhizoboxes. In addition, 100 ml of half-strength

Hoagland's solution was added from above the rhizoboxes (directly into the soil) every 7 days after the start of the experiment to feed the plants (Barbour and DeJong, 1977). Experimental climate chamber (aralab fitoclima 5000 PLH, Riode Mouro, Portugal) temperature ranged from 16 °C to 24 °C and the air humidity ranged from 80% to 64%. The light (cool white fluorescent lamps, Osram, Germany) intensity at plant level was reached up to 750 μmol m^{-2} s^{-1} at 12:00 (Table S1). The experiment lasted for a total of 100 days.

2.3. Sampling

All microenvironmental devices were sampled (i.e., three replicate samples for both soil and root exudates). To aseptically collect the rhizosphere soil, the entire plant was removed from the soil and gently shaken to remove the soil not tightly attached to the root. A pull vibration method was first employed to separate the rhizosphere soil particles which spontaneously detached from the roots. Then, the plants were placed in beakers containing 2 L of physiological solution (9 g L^{-1} NaCl) to obtain the rhizosphere interface, which is the soil closely adhering to the root rhizoplane (Mapelli et al., 2018). The water-soil mixture was vortexed for 5 min and centrifuged at 4000 rpm for 5 min. The supernatant was discarded, and the remaining soil fraction was mixed with the rhizosphere soil previously detached from roots as the rhizosphere soil (Mapelli et al., 2018). Both bulk and rhizosphere soil samples were stored at − 80 °C for molecular analysis.

2.4. Root exudate collection and analysis

After soil sampling, the plant roots were carefully and repeatedly washed with deionized water. These plants were then inserted into test tubes filled with sterile glass beads (providing soil-like mechanical resistance and porosity) (Tückmantel et al., 2017). Then, 60 ml of distilled water was added to the test tube and the root exudate was allowed to secrete for 8 h (Wang et al., 2019). After that, the trap solutions containing exudate collected in each test tube were filtered through a sterile syringe filter (0.45 μm) to remove plant root residues. The trap solution was freeze-dried and weighed. The dried powder was then fully dissolved in 80% methanol solution according to the method described by Zhu et al. (2016). The root exudates were derivatized by adding methoxamine hydrochloride / pyridine and MSTFA (+1% TMCS) according to the method described by Sana et al. (2010). GC-MS analysis of root exudates was performed using a Model 7890 gas chromatograph system (Agilent, Santa Clara, CA) coupled with a Pegasus HT time-of-flight mass spectrometer (Leco, St. Joseph,MI). Data files were subjected to data baseline filtering, baseline calibration, peak alignment, deconvolution analysis, peak identification, and peak area integration using LECO's Chroma TOF 4.3 3x software and Leco- fiehn Rtx5 databases. A total of 256 peaks were detected, in which 178 named metabolites were identified. All detected substances were grouped according to acids, carbohydrates, lipids, alcohols, amines and other metabolites (substances that were not identified were also classified as other metabolites). The acids were further subdivided: firstly, low-molecular-weight organic acids were filtered and classified as organic acids, and the remaining substances were classified as fatty acids, amino acids, and other acids.

2.5. DNA extraction and Illumina sequencing

According to the manufacturer instructions, extractions were carried out on 500 mg of soil (wet weight) using the E.Z.N.A.® soil DNA Kit (Omega Bio-tek, Norcross, GA, U.S.). DNA was extracted from three technical replicates per sample to minimize the DNA extraction bias. The final DNA concentration and purification were determined by NanoDrop 2000 UV–vis spectrophotometer (Thermo Scientific, Wilmington, USA), and DNA quality was checked by 1% agarose gel electrophoresis. The V3-V4 hypervariable regions of the bacteria 16 S rRNA gene were amplified with primers 338 F (5′-ACTCCTACGGGAGGCAGCAG-3′) and 806 R (5′-GGACTACHVGGGTWTCTAAT-3′) by thermocycler PCR system (GeneAmp 9700, ABI, USA). The PCR reactions were conducted using the following program: 3 min of denaturation at 95 °C, 27 cycles of 30 s at 95 °C, 30 s for annealing at 55 °C, and 45 s for elongation at 72 °C, and a final extension at 72 °C for 10 min. PCR reactions were performed in triplicate 20 μL mixture containing 4 μL of 5 × FastPfu Buffer, 2 μL of 2.5 mM dNTPs, 0.8 μL of each primer (5 μM), 0.4 μL of FastPfu Polymerase and 10 ng of template DNA. The resulted PCR products were extracted from a 2% agarose gel and further purified using the AxyPrep DNA Gel Extraction Kit (Axygen Biosciences, Union City, CA, USA) and quantified using QuantiFluor ™ -ST (Promega, USA) according to the manufacturer protocol. Illumina MiSeq high-throughput sequencing was performed at Majorbio Biotech Co., Ltd. Purified amplicons were pooled in equimolar and paired-end sequenced on an Illumina MiSeq platform (Illumina, San Diego, USA) according to the standard protocols by Majorbio Bio-Pharm Technology Co. Ltd. (Shanghai, China). The raw sequences were analyzed using the QIIME2 framework (Bolyen et al., 2019, p. 2). Filtered high-quality reads were analyzed using DEBLUR software to produce amplified sequence variants (ASVs). The taxonomic assignment of ASVs was performed with the classifier in the QIIME2 framework (February 2020).

2.6. Statistical analyses

The means ± standard deviations of three replicates were calculated. Significant differences of mean were detected by one-way analysis of variance with Duncan's multiple range test.

For root exudates, compound-specific concentrations (μg $plant^{-1}$) were calculated using the dry weight of the trap solution multiplied by the relative peak height. Principal component analysis (PCA) and partial least squares discriminant analysis (PLS-DA) of root exudates were performed using R software (v 4.2.0, R Core Team and the R Foundation for Statistical Computing, Vienna, Austria).

For soil microorganisms, the alpha diversity of the samples was obtained using the QIIME2 framework calculations. A principal coordinate analysis (PCoA) was performed using R software to determine β diversity. Co-occurrence networks of microbial communities with different pollution conditions were constructed. Correlations with $\rho > 0.8$ and P values < 0.05 were considered statistically significant and robust. A checkerboard score (C-score) model was used as a measure of species separation and its variance (C_{var}-score) as a measure of species separation and aggregation in the microbial community (Niederdorfer et al., 2021). Co-occurrence network and C-score analysis of the samples were performed using Python and R scripts (https://github.com/RichieJu520). To clarify the functional content of the communities in the samples, predictions were made using the PICRUSt2 tool based on 16 S rRNA gene sequencing data (Douglas et al., 2020a).

The relationships between plant species, PFOS and F-53B concentrations, soil physicochemical properties, root secretion characteristics and soil microbial communities were analyzed using the partial least squares pathway model (PLS-PM) of R software.

3. Results and discussion

3.1. Soil physicochemical properties

Soil total organic carbon (TOC), pH, ammonium (NH_4^+-N), and nitrate (NO_3^--N) were all affected by both PFOS and F-53B exposure (Table 1). The pH of soils with no plant (bulk soil), or planted with Ls or Pc all tended to increase with PFOS or F-53B concentration. The differences in pH of rhizosphere soil of the same plant species were not significant among the treatment groups. The addition of both PFAS did not cause significant ($p > 0.05$) changes in the TOC content of the bulk soils. However, the addition of both PFASs led to an increase in TOC content in both Ls and Pc soils (significantly higher than the respective

Table 1
Chemical properties[a] of bulk and rhizosphere soils under different perfluorooctanesulfonate (PFOS) and chlorinated polyfluoroalkyl ether sulfonate (F-53B) concentrations.

	Control	*Low F-53B*	*Low PFOS*	*High F-53B*	*High PFOS*
pH					
Bulk soil	7.06 ± 0.02^{bA}	7.08 ± 0.02^{bA}	7.08 ± 0.01^{bA}	7.15 ± 0.02^{abA}	7.16 ± 0.01 ^{aA}
Ls rhizosphere soil	6.93 ± 0.02^{aB}	6.93 ± 0.01^{aB}	6.95 ± 0.02^{aB}	6.98 ± 0.01^{aB}	7.01 ± 0.02^{aB}
Pc rhizosphere soil	7.00 ± 0.02^{aAB}	6.98 ± 0.03^{aAB}	7.01 ± 0.02^{aAB}	7.06 ± 0.03^{aAB}	7.07 ± 0.02^{aAB}
TOC (g kg^{-1} dw)					
Bulk soil	15.23 ± 0.78^{aC}	15.02 ± 0.64^{aC}	15.11 ± 0.57^{aC}	15.24 ± 0.10^{aB}	15.33 ± 0.19^{aB}
Ls rhizosphere soil	25.36 ± 0.61^{bA}	29.53 ± 0.78 ^{aA}	28.29 ± 0.11 ^{aA}	26.83 ± 0.43^{abA}	27.36 ± 0.15 ^{aA}
Pc rhizosphere soil	22.79 ± 0.38^{bB}	25.09 ± 0.57^{aB}	24.66 ± 0.80^{abB}	26.19 ± 0.50 ^{aA}	25.84 ± 0.84 ^{aA}
NO_3^--N (g kg^{-1} dw)					
Bulk soil	0.67 ± 0.03^{bA}	0.76 ± 0.03^{abA}	0.42 ± 0.01^{cA}	0.83 ± 0.03 ^{aA}	0.72 ± 0.02^{abA}
Ls rhizosphere soil	0.10 ± 0.02^{aB}	0.11 ± 0.01^{aB}	0.12 ± 0.02^{aB}	0.10 ± 0.03^{aB}	0.09 ± 0.02^{aB}
Pc rhizosphere soil	0.16 ± 0.01^{aB}	0.14 ± 0.01^{abB}	0.13 ± 0.02^{abB}	0.08 ± 0.01^{bB}	0.07 ± 0.02^{bB}
NH_4^+-N (g kg^{-1} dw)					
Bulk soil	1.23 ± 0.02^{eA}	1.25 ± 0.02^{dA}	1.34 ± 0.02^{cA}	1.54 ± 0.02^{bA}	1.82 ± 0.01 ^{aA}
Ls rhizosphere soil	0.21 ± 0.01^{bB}	0.19 ± 0.02^{bB}	0.23 ± 0.02^{bB}	0.35 ± 0.02^{aB}	0.38 ± 0.01^{aB}
Pc rhizosphere soil	0.23 ± 0.02^{aB}	0.21 ± 0.02^{aB}	0.19 ± 0.02^{aB}	0.27 ± 0.02^{aB}	0.27 ± 0.02^{aC}

[a] Results are presented as means ± standard deviations (n = 3); different lowercase letters indicate statistically significant ($p < 0.05$) differences between treatments (control, low F-53B, low PFOS, high F-53B and high PFOS) in the same soil; different uppercase letters indicate statistically significant ($p < 0.05$) differences between soils (bulk soil, Ls and Pc rhizosphere soil) under the same treatment. Ls: *Lythrum salicaria*; Pc: *Phragmites communis*; dw: dry weight.

controls except for Ls soils in the high F-53B group and Pc soils in the low PFOS group), while F-53B resulted in a greater magnitude of TOC content change. This may be because plants release more exudates for defense against PFASs (in fact, the dry weight of root exudates increased with increasing PFOS/F-53B treatment concentration, Fig. S5), which leads to the increase of TOC in rhizosphere soil. The NO_3^--N content in the three soils showed different trends with increasing PFOS concentrations (bulk soils: significantly decreasing and then significantly increasing, Ls soils: no significant change, and Pc soils: decreasing). The NO_3^--N content in bulk soils increased with increasing F-53B concentration, while the trend of NO_3^--N content in both rhizosphere soils with increasing F-53B concentration was similar to that of PFOS. The NH_4^+-N content in both bulk soils increased with significantly increasing PFOS or F-53B concentrations. It could be found that PFOS (increased by 8.94–45.97%) had a more significant effect on NH_4^+-N content in both soils compared to F-53B (increased by 1.63–25.20%) in bulk soils. In Ls soils, high PFOS or F-53B concentrations caused a significant ($p < 0.05$) increase in NH_4^+-N content. In contrast, neither of the two PFAS additions caused significant changes in NH_4^+-N in Pc soils. In experiments on activated sludge, PFOS has been shown to alter the microbial community structure and affect the performance of activated sludge in both acute and long-term exposures (Lu et al., 2022; Sheng et al., 2021). The differences in the bulk soil properties likely result from both the direct effects of PFAS and the indirect effects mediated by PFAS-affected microbial communities. Moreover, it can be found that there are differences between properties of bulk soils exposed to PFOS and F-53B. Some of the available literature suggests that the bioconcentration and toxicity of these two PFASs are different (Liu et al., 2018; Tu et al., 2019). The varied trends of soil properties with increasing PFAS concentration between rhizosphere and bulk soil indicate that the effects of PFAS on soil are also related to the presence or absence of plants. We previously investigated the effects of PFOS on N cycling rates and N-related functional gene expression in soils and found that plants actively limit the steps of N cycling in rhizosphere soils leading to the accumulation of NH_4^+-N and the reduction of NO_3^--N (Lu et al., 2020a). This was corroborated in the present study and a similar phenomenon was observed in the F-53B experimental group, suggesting that plants might also down-regulate the rate of N cycling in their rhizosphere soils during the defense against F-53B. Previous literature has shown that the uptake kinetics of PFAS by plants are influenced by soil properties such as pH (W. L. Wang et al., 2020; W. Wang et al., 2020; Zhao et al., 2013). Our previous study found that trace amounts of PFAS did not have entirely adverse effects on certain plants (Qian et al., 2019). Therefore, we speculate that plants may have different physiological responses to various doses of PFAS. That is, plants modify PFAS uptake kinetics by altering root exudation through feedback regulation to adjust soil physicochemical properties directly or indirectly by affecting rhizosphere microorganisms.

3.2. Root exudate metabolomics

Studies have found that plants release 11–40% of the net product of photosynthesis to the rhizosphere (Huang et al., 2019; Morgan et al., 2005; Walker et al., 2003). Root exudates of plants play a crucial role in regulating plant-environment interactions (Lakshmanan et al., 2014; Singh et al., 2004). The PFASs have been reported to cause oxidative stress in plants resulting in phytotoxicity (Li et al., 2022; Qian et al., 2019; Qu et al., 2010). Therefore, it is desirable to know whether exposure to different levels of PFOS and F-35B has altered the root metabolite profile. A total of 178 root exudates were identified by GC-MS analysis followed by classification according to their chemical properties (i.e., acids, carbohydrates, lipids, alcohols, amines and other metabolites, Fig. 1a). The composition of Ls root exudate was more susceptible to the exposure of PFASs compared to that of Pc. The acids proportion in the root exudate of both plants was elevated with exposure to the PFASs. The percentage of acids in the root exudates of Ls and Pc under the influence of high PFOS and Pc under the influence of high F-53B was significantly ($p < 0.05$) higher than that of the respective controls (Fig. S4). In contrast, the percentage of carbohydrates in the root exudate of Ls significantly increased under the influence of high PFAS concentrations while Pc decreased (significant under high F-53B treatment). The results of fresh weight measurements on plants (Fig. S3) showed that the application of PFOS or F-53B negatively affected plant growth. The fresh weight of both plants in the high concentration group was significantly lower than that of the control group. Carbohydrates accumulate under stress (P. Liu et al., 2020; W. Liu et al., 2020), and in this study, plants were subjected to PFOS or F-53B stress with growth inhibition, leading to a decrease in carbon demand, which resulted in carbohydrate accumulation. This may be one of the reasons for the increase in carbohydrate share of Ls root exudates. Some carbohydrates in root exudates occur primarily passively by diffusion (Bertin et al., 2003), while both PFOS and F-53B have been shown to interact positively with biofilms (Liu et al., 2018). This is one of the reasons for the increase in carbohydrates in metabolites. In addition, some carbohydrates play an active role in root penetration and defense processes (as lubricants) (Galloway et al., 2020) as well as in the activity and metabolism of rhizosphere microorganisms (Meier et al., 2017; Wu et al., 2017). Carbohydrates are the main product of photosynthesis in plants; therefore, the weakening of carbohydrate metabolism may be related to the disruption of plant photosynthetic pigments by PFASs (Li et al., 2021). In addition, differences in the carbon investment strategies of plants to the root system in different environments may also be responsible (Zhang et al., 2017). The results imply that Ls and Pc adopted different

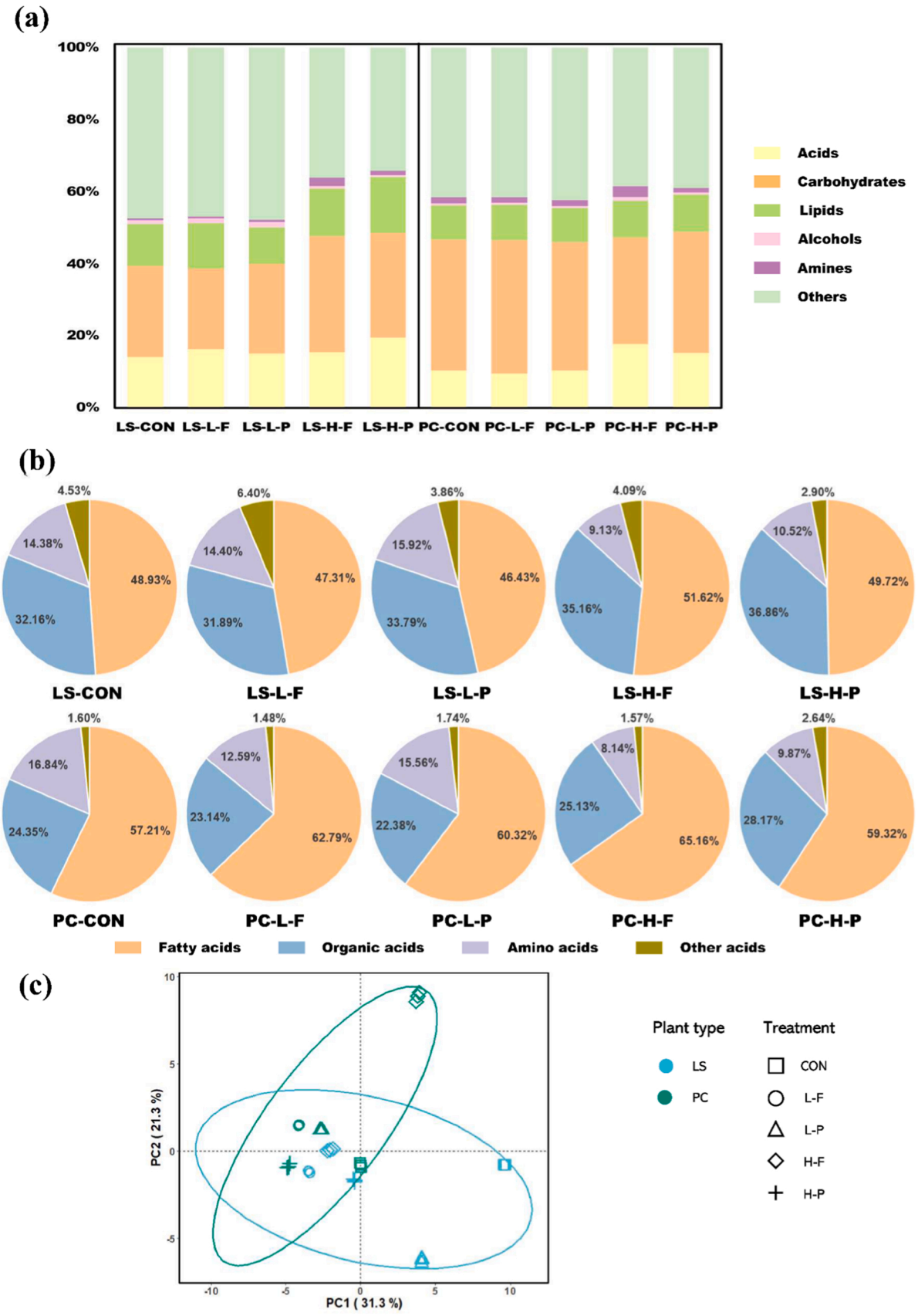

Fig. 1. Effects of different concentrations of perfluorooctanesulfonate (PFOS) and chlorinated polyfluoroalkyl ether sulfonate (F-53B) on root metabolites of two study plants. The classification and percentage of known (a) metabolites and (b) acids in each sample. (c) Score scatter plot of PCA model for identified differential metabolites. LS: *Lythrum salicaria*; PC: *Phragmites communis*; CON: no addition; L: low concentration; H: high concentration; P: PFOS; F: F-53B.

strategies to respond to the same environmental stress, mirroring previous studies that reported different responses and sensitivity of monocotyledonous and dicotyledonous to certain abiotic stresses (Corrales et al., 2008; Huang et al., 2011). The high concentration of PFOS led to a significant ($p < 0.05$) increase in the percentage of lipids in the metabolites of Ls root exudates, while the changes in the percentage of lipids were insignificant in any of the other experimental groups. Disruption of plant cell membranes by external stress results in an increase in lipids in metabolites (Lucini et al., 2019). In addition, some lipids act as signaling and defense substances in plants (Suarez-Fernandez et al., 2020), and the increase in the percentage of lipids implies the initiation of plant defense mechanisms. Wen et al. (2016) reported that the content of lipids was negatively correlated with the accumulation of PFOS, suggesting that plants tend to reduce the accumulation of pollutants by increasing lipids. The percentage of lipids in root exudates did not change significantly under the influence of F-53B, implying that plants did not adopt the same defense strategy in response to F-53B as they did in response to PFOS. Neither PFOS nor F-53B resulted in significant changes in the percentage of alcohols in the root exudates of the two plants. The relative abundance of amines in the root exudates of both plants was significantly ($p < 0.05$) increased only in the high F-53B treatment group. According to Jones et al. (2003), amines in root exudates are used for microbial growth, and the increase in amines would lead to an increase in NH_4^+-N in the rhizosphere soil (Table 1). Wang et al. (2021) suggested that the increase in amines in plant root exudates under stress may be related to the massive degradation of proteins in plants during stress resistance.

Many acids play an essential role in growth regulation and defense processes in plants (Badri and Vivanco, 2009; Bertin et al., 2003). In our study, the proportion (not significant, Fig. 1b and S6) and amount (significant, $p < 0.05$, Fig. S7) of fatty acid in the root metabolites increased due to exposure to high concentrations of PFOS and F-53B. Fatty acids play a role in plant growth regulation (Bertin et al., 2003) and are often used as indicators of root membrane damage (Rico et al., 2013; Wang et al., 2019). An increase in fatty acid metabolism protects plants from reactive oxygen species (Wang et al., 2019). Bertin et al. (2003) suggested that root secretion of amino acids occurs mainly passively by diffusion and might be enhanced under stress. However, in our study, the amino acids secreted by plants exposed to PFOS and F-53B were lower than the control group (Fig. 1b, S6 and S7). A recent study showed that PFOS led to a decrease in the amino acids content of the leaves (Guo et al., 2020). Amino acids are essential components of proteins, metabolite precursors and signaling molecules and play an important role in plant stress tolerance by regulating intracellular pH, stomatal conductance and detoxifying reactive oxygen species (Fotiadis et al., 2013; P. Liu et al., 2020; W. Liu et al., 2020). Several phytotoxicological experiments have observed increased soluble proteins in plant roots affected by PFASs (Li et al., 2022). Zhang et al. (2012) suggested that the affected biosynthesis of substances such as proteins leads to a decrease in free amino acids. This may be one of the reasons for the significant decrease in amino acids after exposure to PFOS/F-53B. Organic acids released from plant cells positively correlate with plant stress tolerance to biotic and abiotic stresses (Upchurch, 2008). In the present study, the organic acids in the root metabolites of Ls were upregulated generally with the increasing concentration of PFOS/F-53B (Fig. S7). However, exposure to low concentrations of both PFASs resulted in a decrease in the content of organic acids in the Pc root system but an increase observed under high stress (Fig. S7). Studies have suggested that organic acid from roots release can operate by a variety of mechanisms in response to many well-defined environmental stresses (Jones, 1998; Panchal et al., 2021). This suggests that these two types of plants are different in their tolerance to stress or that these two types of plants have different stress tolerance strategies. Surprisingly, of the organic acid, the abundance of citric acid in the root exudates of both plants decreased significantly ($p < 0.05$) and then increased significantly ($p < 0.05$) with increasing PFOS concentration, while it showed a significant ($p < 0.05$) up-regulation and then significant ($p < 0.05$) down-regulation trend with increasing F-53B concentration. Changes in citric acid content were possibly a metabolic shift in the tricarboxylic acid cycle (Badri and Vivanco, 2009) or may have accelerated the uptake of certain elements by the plant (Zhao et al., 2016). Studies have shown that root-released acids (e.g. malic and citric acids) attract certain specific strains (de Weert et al., 2002), and in this study both PFAS resulted in significant ($p < 0.05$) up-regulation of malic acid.

The PCA of the metabolomics data produced two principal components (PCs) which explained more than 50% of the total variance (PC1 and PC2 explained 31.3% and 21.3%, respectively). The score plots (Fig. 2c) of PC1 and PC2 showed that the root exudate of Ls changed more significantly under the influence of both PFASs, while the change in root exudate of Pc was not as evident in all treatments except the high concentration of F-53B. To visualize the general differences, the identified metabolites were normalized and analyzed by partial least squares discriminant analysis (PLS-DA). Both plant species and treatment types showed a clear separation (Fig. S8).

3.3. Structure and function pattern of microorganisms

The Shannon index was used to assess the microbial diversity in the rhizosphere soil and bulk soil after exposure to PFOS and F-53B. In bulk soils, soil microbial community Shannon index was significantly ($p < 0.05$) reduced by low concentrations of F-53B and further reduced substantially with increasing F-53B concentrations (Fig. 2a). Previous studies have shown that some PFASs cause a reduction in microbial diversity in sediments or activated sludge (Lu et al., 2022; Qiao et al., 2018; Sun et al., 2016). In contrast to F-53B, the addition of low concentrations of PFOS in the bulk soil resulted in a significant increase in the mean value of the Shannon index and with increasing PFOS concentration the mean value of the Shannon index decreased. The degree of variation in the alpha diversity index of microbial communities in plant rhizosphere soils was significantly smaller than in bulk soils due to the action of plants (Fig. 2a). A number of studies have found that root exudates play a role in stabilizing or directing the structure of the soil microbial community during stress (Li et al., 2019; Liao et al., 2021; Louvel et al., 2011). The trend of the Shannon index of microbial communities in the rhizosphere soil of the two studied plants under the influence of PFOS followed that of the bulk soil, i.e., it increased first and then decreased. Similar to bulk soils, low concentrations of F-53B led to a reduction in the alpha diversity index of microbial communities in rhizosphere soils. However, the alpha diversity index did not decrease further with increasing F-53B concentrations. Studies of plant-microbe interactions have shown that plants are able to shape their rhizosphere microbial communities according to the environment (pathogens, nutrient deficiencies, pollutant stress, etc.) they are exposed to (Berendsen et al., 2012). Differences in the alpha-diversity of microbial communities in bulk and rhizosphere soils imply the recruitment of microorganisms by plants; whereas differences in the alpha-diversity of microbial communities in rhizosphere soils due to PFOS and F-53B imply differences in the recruitment of microorganisms by plants in different environments (i.e., different responses of rhizosphere defense systems). Multivariate ordination PCoA of community beta-diversity indicates changes within the community (Fig. 2b). The PCoA1 (36.76%) and PCoA2 (27.64%) described a total of 64.40% variation in microbial community composition. The PCoA plots of ASVs-based samples showed that the samples containing varying quantities and types of PFAS were dispersed and independently distributed along the PCoA2 axis. And the PCoA1 axis mainly distinguished the Ls rhizosphere soil samples affected by low PFOS concentrations from other samples. The alpha diversity analysis (Fig. 2a) showed that microbial diversity in the rhizosphere soil of Ls affected by low concentration of PFOS was not significantly different from that in the control, and in high concentration of PFOS and F-53B groups. These results indicated that the microbial community structure in the rhizosphere of Ls varied greatly under the

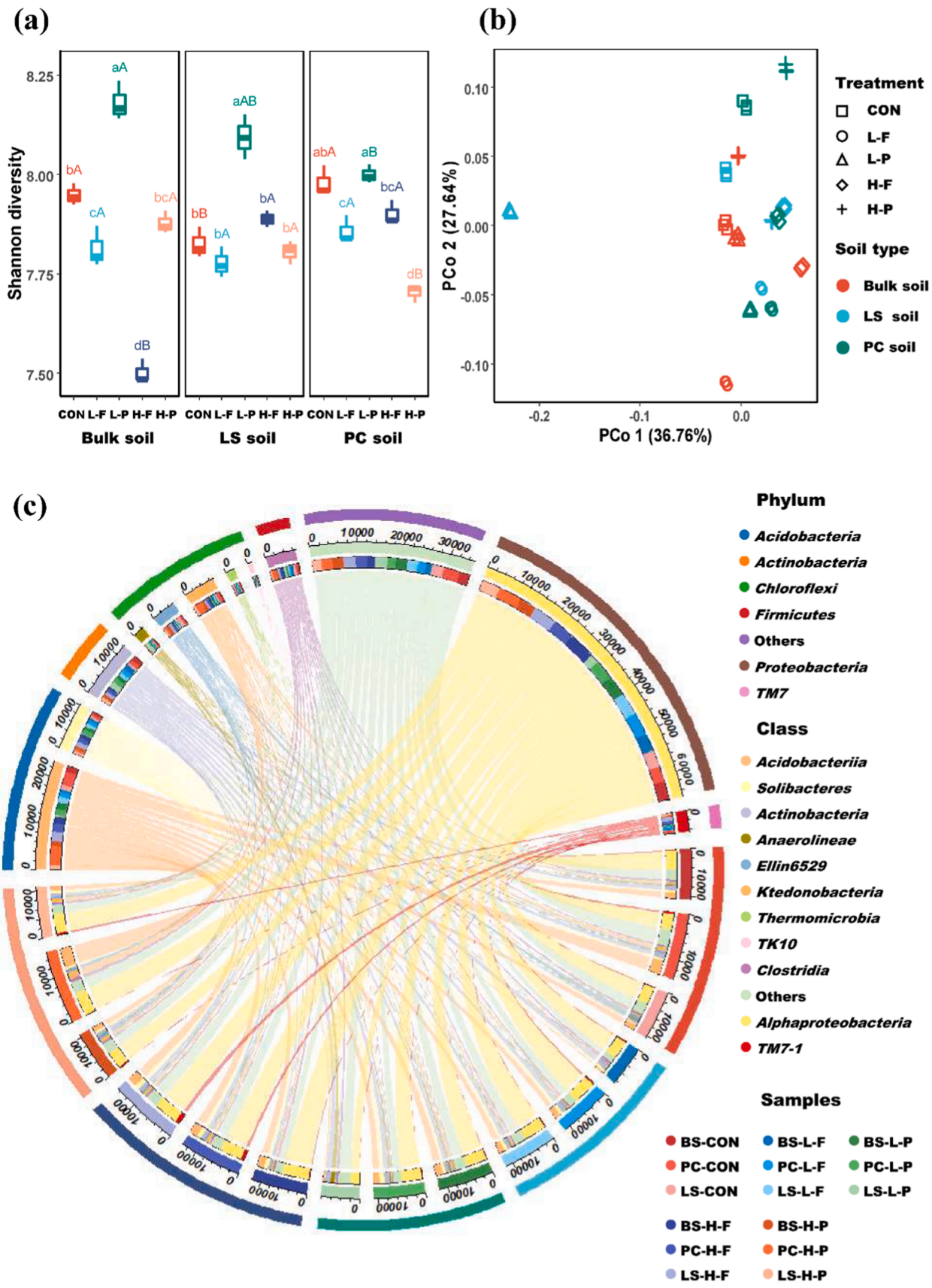

Fig. 2. The shift of microbial community diversity, structure and composition in soils in each group according to the 16 S rRNA data. (a) The Shannon alpha diversity estimators for the samples; lowercase letters indicate significant ($n = 3$, $p < 0.05$) differences between treatments from the same soil; uppercase letters indicate significant ($n = 3$, $p < 0.05$) differences between soils of the same treatment. (b) Principal coordinates analysis (PCoA) plot of soil microbiomes based on weighted UniFrac distance, % variance explained is shown in parentheses. (c) The chord diagram shows the taxonomic composition of microbial at phylum and class.

influence of low concentrations of PFOS. Previous studies have found that nitrogen cycling capacity and nitrogen functional gene abundance in Ls rhizosphere are highly affected by PFOS (Lu et al., 2020b). The results of the present study imply that this is related to changes in microbial community structure. Interestingly, the Ls root exudates samples affected by low PFOS in the PCA analysis (Fig. 1c) displayed a clear separation from the other samples as well. And permutational multivariate analysis of variance (PERMANOVA) analysis (Table S2) showed that the root exudates of the low PFOS group were significantly different from the control, high PFOS and high F-53B groups. This further suggests that root exudates guide changes in the structure of the rhizosphere microbial community.

A total of 29 phyla were identified by the amplicons, and their abundance varied among samples. Fig. 2c shows the classes with > 1% abundance and the phylum they belong to. Phylum level analysis showed that *Proteobacteria* was generally the most dominant phylum, irrespective of the treatments. With the exposure to F-53B, *Proteobacteria* increased by 21.90–30.05% in the bulk soil compared to the control; while only in the high PFOS environment *Proteobacteria* decreased slightly by 7.78% compared to the control. Regulated by Ls root exudates, the percentage of *Proteobacteria* increased significantly under low F-53B, decreased significantly under low PFOS, and returned to the control level under high F53-B/PFOS. In Pc rhizosphere soils, both types of PFAS tested resulted in a significant increase and then a significant decrease in *Proteobacteria* percentage with exposure concentration. *Proteobacteria*, one of the largest bacterial phyla among prokaryotes (Gupta, 2000), are ubiquitous in the soil environment and closely associated with nutrient cycles such as nitrogen (Kong et al., 2013). Researchers have found that some Gram-negative bacteria with thin cell walls and complex ingredients in *Proteobacteria* can respond rapidly to stress and then tolerate contamination (L. W. Wang et al., 2020; L. Wang et al., 2020). Moreover, the proportion of *Pseudomonas* (belonging to *Proteobacteria*) in the rhizosphere of both plant species increased significantly at high PFAS concentrations. Kim et al. (2012) found that some Pseudomonas strains can efficiently remove the -CF_2- group, which hints at plant microbial recruitment strategies. At the phylum level, the abundance of *Acidobacteria*, *Chloroflexi*, *Actinobacteria*, and *Firmicutes* was successively after *Proteobacteria* in each sample, in total accounting for 75.70–87.31% of the whole community (including *Proteobacteria*), in line with the previous studies on the investigation of soil microbial communities by PFASs (Bao et al., 2018; Cai et al., 2020; Qiao et al., 2018). The relative abundance of *Proteobacteria* as a copiotrophic taxon usually increases in high trophic environments, while the relative abundance of oligotrophic taxa (mainly *Acidobacteria*) shows the opposite pattern (Fierer et al., 2012), which is consistent with the relative abundance behavior of both phyla of bacteria in the present study. It is worth noting that in a study examining the interaction between PFASs and simplified bacterial membranes modeled on phospholipid Langmuir monomolecular membranes, Gram-positive bacteria were found to be more resistant to these substances due to their cell membrane structure (Wójcik et al., 2018). The *Actinobacteria*, a phylum of mostly Gram-positive bacteria, did not show an increase in abundance and percentage in bulk soils under the influence of high concentrations of PFOS or F-53B. The same was true for the variation in the abundance of *Actinobacteria* in Pc rhizosphere soils. However, the abundance of *Actinobacteria* in the rhizosphere soil of Ls was significantly increased, especially the abundance of *Actinobacteria* in the low PFOS group was 4.08 times higher than that in the control group. This clearly indicates that the effect of PFASs on the soil microbial community is plant-specific.

Networks were constructed from the strong and significant correlation of Spearman's rank coefficients, which led to further analysis to explore the community co-occurrence patterns. The networks for each treatment differed substantially in the number of nodes (ASVs), number of edges (connections), modularity (the degree to which species interactions are organized into modules or subnetworks), and clustering coefficients (the degree to which nodes are clustered together) (Fig. 3). In terms of the topological properties of each network, the low PFOS treatment group network has the highest number of nodes and edges, while the high PFOS and high F-53B treatment group networks account for a relatively low number of nodes and edges. And the modularity of the high F-53B and low F-53B treatment group networks were the lowest (0.203) and the highest (0.631), respectively. In a network, a module is a set of highly self-connected ASVs, but is much less connected to ASVs outside the group (Sun et al., 2021). In the control group, the effect of soil (bulk soil, Pc soil or Ls soil) on soil communities was evident in the soil network with multiple discrete modules containing ASVs specific to particular soils. And as PFASs were added, these discrete modules were gradually connected to other modules. This demonstrated that the changes in soil environment caused by the addition of PFASs influenced the co-occurrence trend of different species. Based on the symbiotic network study results, the null model was applied to infer the ecological species interactions in different environments in the microbial community. It can be found that the networks with high concentrations of PFASs had higher C-score standardized effect size (SES) value, while the networks with low concentrations of PFASs had lower C-score SES values. This demonstrated that high concentrations of PFASs increased the degree of species segregation. According to the C_{var}-score SES values, the high concentration of PFOS creates the greatest degree of species segregation and aggregation (Fayle et al., 2013). Furthermore, the results suggest that positive and negative interactions between organisms play important roles in the species segregation of soil microbial communities, with greater contribution of positive interactions in the high PFAS group (C_{var}-score SES: positive> negative, data not shown), but greater contribution of negative interactions in the low and no PFAS groups (C_{var}-score SES: negative> positive, data not shown) (Hu et al., 2017).

To explore the effects of PFOS and F-53B on soil microbial functions, PICRUSt2 was employed to predict functional abundances based on 16 S rRNA gene sequencing data (Douglas et al., 2020b, 2020a). We followed the functional set enrichment analysis described in P. W. Liu et al. (2020); P. Liu et al. (2020) and found significantly (false discovery rate q-value < 0.05) enriched community functions of all soil samples (Fig. 4a). Linear discriminant analysis (LDA) score threshold greater than 2.0 was then set for linear discriminant analysis effect size (LEfSe) analysis to detect feature abundance of soils subjected to different PFOS or F-53B levels (Fisher, 1936)(Fig. 4b). As shown in Fig. 4b and Table S3, there were also significant differences in the functions of the microbial communities between the groups. The bulk soils affected by high concentrations of F-53B had the maximum number of significantly different feature functions among all experimental samples. These differential metabolic pathways were focused on metabolism (many pathways related to substance synthesis) and human diseases (many pathways related to drug resistance). The second highest number of significantly different pathways in Ls soil affected by low concentrations of PFOS was 38. The scores of ko01230 (biosynthesis of amino acids) and ko02010 (membrane transport) ranked first and second, respectively. These pathways are essential for organism growth (Li et al., 2020), illustrating the high microbial recruitment of Ls under the impact of PFOS at low concentrations. Furthermore, according to the predicted results, except for Ls rhizosphere soils affected by high PFOS concentrations, the microbial communities in all rhizosphere soil samples had functional pathways with significant differences in abundance between groups. This suggests that the type and concentration of PFASs, as well as the plant species, together influence the function of soil microbial.

3.4. Response strategies of rhizosphere defense system

The question of how PFOS and F-53B impacted the plant rhizosphere defense system, through direct and indirect effects on root exudate secretion and rhizosphere soil microorganisms, was explored by PLS-PM (Fig. 5). It is clear that the plant rhizosphere defense system responded

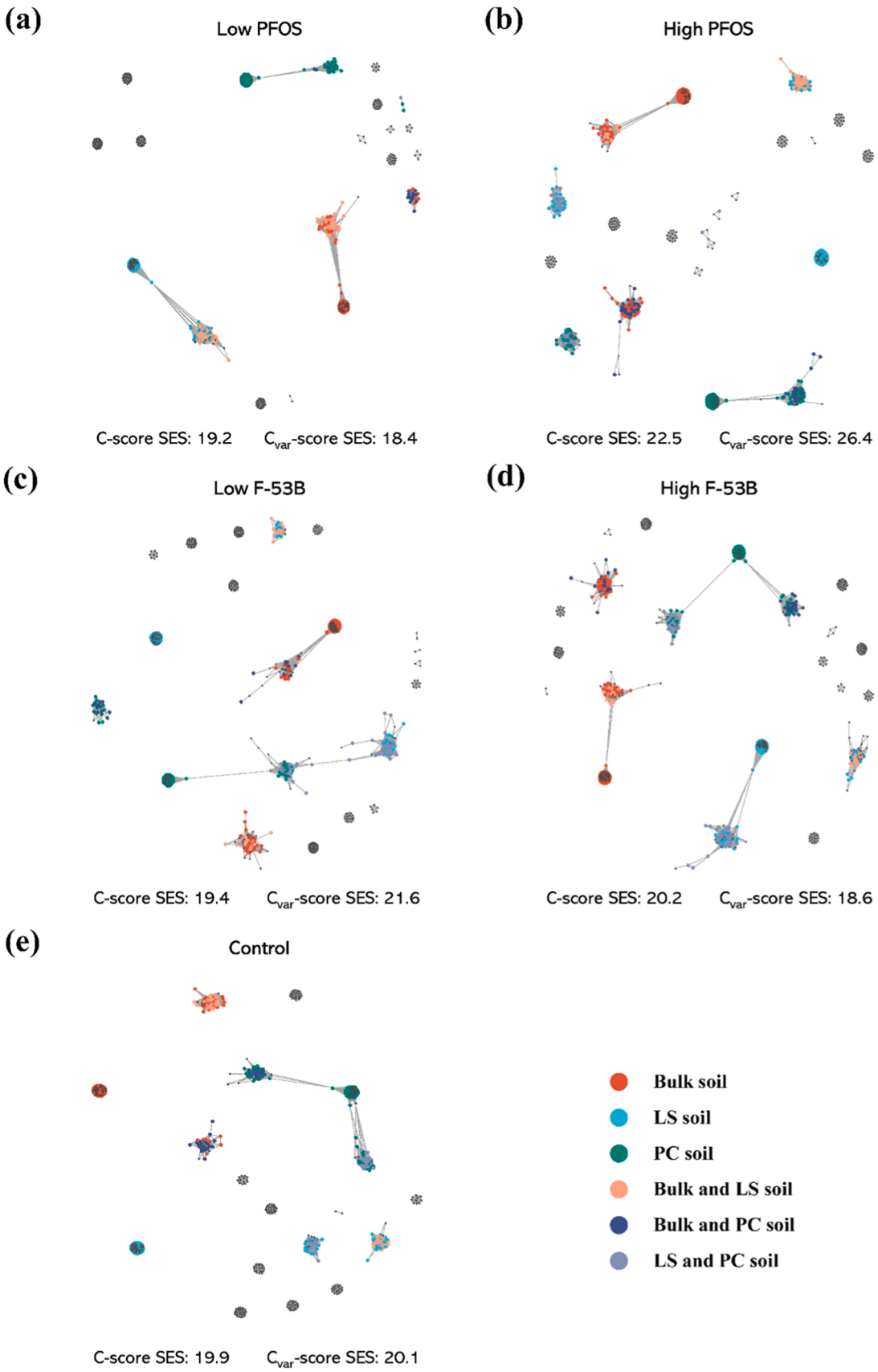

Fig. 3. Co-occurrence patterns of perfluorooctanesulfonate (PFOS) and chlorinated polyfluoroalkyl ether sulfonate (F-53B) concentration-sensitive ASVs. Co-occurrence networks visualizing significant correlations between ASVs in (a) low concentration PFOS soils, (b) high concentration PFOS soils, (c) low concentration F-53B soils, (d) high concentration F-53B soils and (e) uncontaminated soils. OTUs are colored by their association with the different treatment groups.

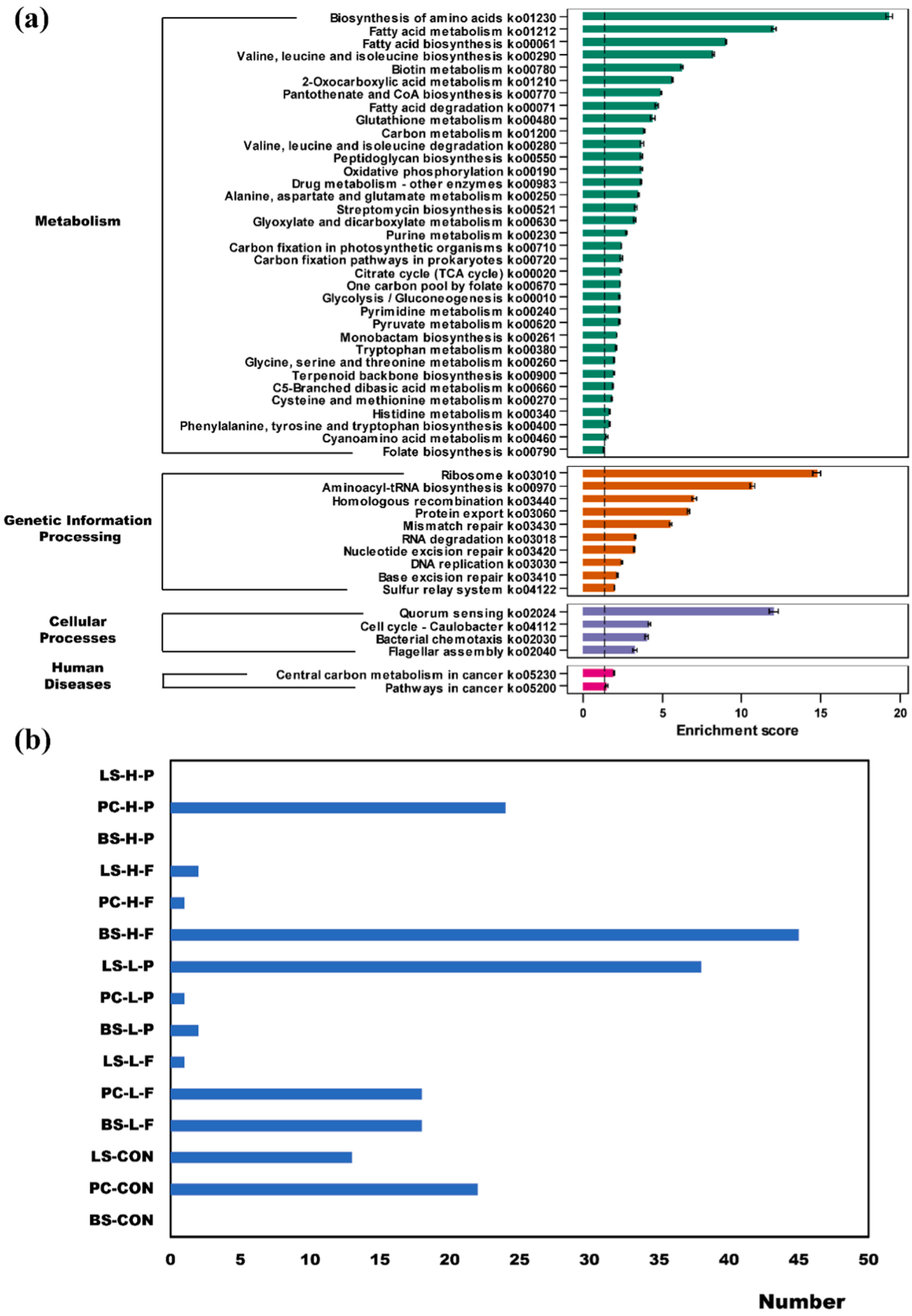

Fig. 4. Prediction of microbial community function in soils. (a) Enrichment analysis of predictive KEGG metabolic modules for microorganisms in all samples. The dashed line indicates that the false discovery rate (FDR) q-value= 0.05. (b) The number of significantly enriched metabolic pathways in each sample was analyzed by linear discriminant analysis (LDA) effect size (LEfSe). LS: *Lythrum salicaria*; PC: *Phragmites communis*; CON: no addition; L: low concentration; H: high concentration; P: perfluorooctanesulfonate (PFOS); F: chlorinated polyfluoroalkyl ether sulfonate (F-53B).

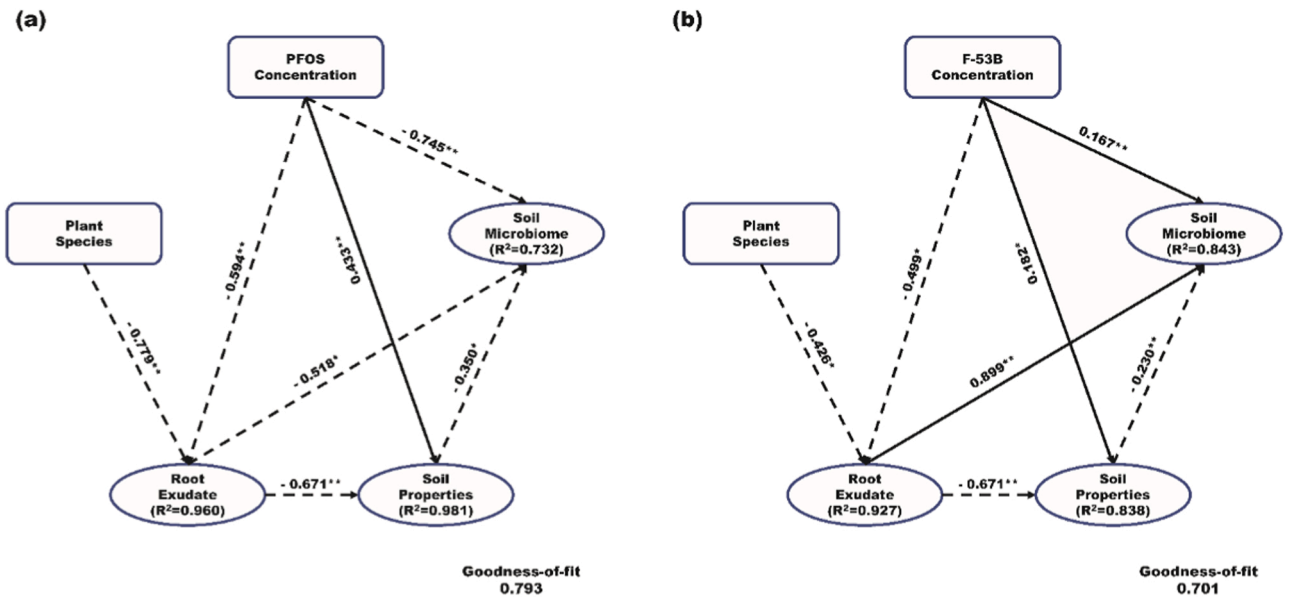

Fig. 5. Partial least squares path modeling (PLS-PM) analysis of the direct and indirect role of PFOS, F-53B and plant species on plant root exudates and rhizosphere microorganisms. Path coefficients are the values next to the lines, the dashed lines indicate negative path coefficients, the solid lines indicate positive path coefficients, and R^2 means the coefficients of determination. Significance levels are indicated: * $P < 0.05$, * * $P < 0.01$.

differently to PFOS and F-53B. The plant species and the concentration of PFOS/F-53B together influenced the fraction and composition of root exudates. Many studies have shown that monocots and dicots exhibit different physiological responses when subjected to abiotic stresses and attribute the cause mainly to differences in cell membrane and structure (Corrales et al., 2008; Piršelová et al., 2011). In addition, recent studies have found that monocots and dicots differ in their defense-gene expression when subjected to stresses (Tolba et al., 2021). This implies that different plants have different defense strategies under the same stress scenario, which was confirmed by our study. In other aspects, different plants also adopt different survival strategies; for example, some plants with rapid belowground resource acquisition strategies are expected to build long and thin roots with minimal biomass investment but high metabolic rate, and plants with slow growth strategies are expected to have longer lifespan and longer return on investment by building thicker and denser roots (Bergmann et al., 2020). Moreover, the microbial community in the rhizosphere soil was influenced by a combination of PFOS/F53B, plant root exudates, and soil physicochemical properties. It is interesting to note that the rhizosphere defense system appears to be less responsive to F-53B compared to PFOS. In particular, for soil microorganisms, the ratio of the path coefficient of concentration to microbial community and the path coefficient of root exudates to microbial community was 1.438 in PFOS-contaminated soils, whereas in F-53B-contaminated soils, the value was only 0.186. A toxicological study on algae reported that F-53B was more destructive to cells compared to PFOS (Liu et al., 2018). It can be inferred that F-53B may have a greater impact on the community structure. This was demonstrated in our experiments (Fig. 2a), where the addition of high concentrations of F-53B in the bulk soil led to greater changes in soil alpha diversity. However, in rhizosphere soils, the small changes in the community structure alpha diversity (Fig. 2a) of microorganisms affected by F-53B were mainly dominated by root exudates (Fig. 5b). In rhizosphere soils, the effect of F-53B was mainly in the root exudates, where the ratio of its concentration to the path coefficient of plant species reached 1.171, while PFOS was only 0.763. Furthermore, we found that the effects of PFOS and F-53B on the soil microbial community (either directly or indirectly) were opposite. This is sufficient to suggest that the environmental impact of F-53B is different from that of PFOS and that it should be treated independently rather than just as a substitute with similar properties to PFOS.

4. Conclusions

This study showed that the addition of PFOS and F-53B led to changes in the fraction and content of plant root exudates. High concentration of F-53B resulted in a significant increase in the percentage of carbohydrates and amines in Ls root exudates, and led to a significant increase in the percentage of acids and amines but a significant decrease in the percentage of carbohydrates in Pc root exudates. High PFOS concentrations significantly increased the percentage of acids, carbohydrates and lipids in the root exudates of Ls and the percentage of acids in the root exudates of Pc. In addition, PFOS and F-53B led to changes in soil physicochemical properties and microbial communities in the bulk soil and both test plant rhizosphere soils. The α-diversity of microbial communities in bulk soils decreased with increasing F-53B concentration and showed a trend of increasing and then decreasing with increasing PFOS concentration. The plants affected by PFOS/F-53B reduced the effect of hazardous substances on the α-diversity of microbial communities in rhizosphere soils to some extent. Besides, the complex regulatory mechanisms of plants lead to different response strategies of rhizosphere defense systems in different plant species, which deserve further investigation. These findings provide insights involving bioremediation and other hazardous substance management approaches.

Environmental implication

Perfluorooctanesulphonicacid (PFOS) and its substitutes Chlorinated polyvinyl fluoride ether sulfonates (trade name F-53B) are widely found in the environment and have been shown to have potentially biotoxic effects. However, there are no relevant studies on the response of plant rhizosphere defense systems to F-53B or PFOS. This work explored the potential environmental hazards of these two substances and the response strategies of plant rhizosphere defense systems from the perspectives of plant root metabolites and microbial community structure. The results are of great use to environmental agencies and regulatory bodies.

CRediT authorship contribution statement

Bianhe Lu: Conceptualization, Methodology, Writing – original

draft, Investigation. **Jin Qian:** Supervision, Validation. **Jing Hu:** Writing – review & editing, Formal analysis. **Yuanyuan Huang:** Writing – review & editing, Formal analysis. **Peifang Wang:** Resources, Data curation. **Junwei Shen:** Software, Visualization. **Yuxuan He:** Investigation. **Sijing Tang:** Investigation. **Yin Liu:** Investigation. **Yuhang Zhang:** Investigation.

Declaration of Competing Interest

The authors declare that they have no known competing financial interests or personal relationships that could have appeared to influence the work reported in this paper.

Data Availability

Data will be made available on request.

Acknowledgments

This study was supported by the National Natural Science Foundation of China (No. 51779078), the Six Talent Peaks Project in Jiangsu Province (No. JNHB-012), the Fundamental Research Funds for the Central Universities, and the World-Class Universities (Disciplines), and the Characteristic Development Guidance Funds for the Central Universities, the Project supported by the National Key Plan for Research and Development of China (2016YFC0401703), the National Major Projects of Water Pollution Control and Management Technology (No. 2017ZX07204003), and Priority Academic Program Development of Jiangsu Higher Education Institutions (PAPD).

Appendix A. Supporting information

Supplementary data associated with this article can be found in the online version at doi:10.1016/j.jhazmat.2022.130119.

References

Abdel-Gawad, F.Kh, Khalil, W.K.B., El-Kady, A.A., Waly, A.I., Abdel-Wahhab, M.A., 2016. Carboxymethyl chitosan modulates the genotoxic risk and oxidative stress of perfluorooctanoic acid in Nile tilapia (Oreochromis niloticus). J. Saudi Soc. Agric. Sci. 15, 57–66. https://doi.org/10.1016/j.jssas.2014.04.005.

Badri, D.V., Vivanco, J.M., 2009. Regulation and function of root exudates. Plant Cell Environ. 32, 666–681. https://doi.org/10.1111/j.1365-3040.2009.01926.x.

Baetz, U., Martinoia, E., 2014. Root exudates: the hidden part of plant defense. Trends Plant Sci. 19, 90–98. https://doi.org/10.1016/j.tplants.2013.11.006.

Bao, Y., Li, B., Xie, S., Huang, J., 2018. Vertical profiles of microbial communities in perfluoroalkyl substance-contaminated soils. Ann. Microbiol. 68, 399–408.

Barbour, M.G., DeJong, T.M., 1977. Response of west coast beach taxa to salt spray, seawater inundation, and soil salinity. Bull. Torre Bot. Club 104, 29–34. https://doi.org/10.2307/2484662.

Berendsen, R.L., Pieterse, C.M.J., Bakker, P.A.H.M., 2012. The rhizosphere microbiome and plant health. Trends Plant Sci. 17, 478–486. https://doi.org/10.1016/j.tplants.2012.04.001.

Bergmann, J., Weigelt, A., Plas, F., van der, Laughlin, D.C., Kuyper, T.W., Guerrero-Ramirez, N., Valverde-Barrantes, O.J., Bruelheide, H., Freschet, G.T., Iversen, C.M., Kattge, J., McCormack, M.L., Meier, I.C., Rillig, M.C., Roumet, C., Semchenko, M., Sweeney, C.J., Ruijven, J., van, York, L.M., Mommer, L., 2020. The fungal collaboration gradient dominates the root economics space in plants. Sci. Adv. https://doi.org/10.1126/sciadv.aba3756.

Bertin, C., Yang, X., Weston, L.A., 2003. The role of root exudates and allelochemicals in the rhizosphere. Plant Soil 256, 67–83. https://doi.org/10.1023/A:1026290508166.

Bolyen, E., Rideout, J.R., Dillon, M.R., Bokulich, N.A., Abnet, C.C., Al-Ghalith, G.A., Alexander, H., Alm, E.J., Arumugam, M., Asnicar, F., Bai, Y., Bisanz, J.E., Bittinger, K., Brejnrod, A., Brislawn, C.J., Brown, C.T., Callahan, B.J., Caraballo-Rodríguez, A.M., Chase, J., Cope, E.K., Da Silva, R., Diener, C., Dorrestein, P.C., Douglas, G.M., Durall, D.M., Duvallet, C., Edwardson, C.F., Ernst, M., Estaki, M., Fouquier, J., Gauglitz, J.M., Gibbons, S.M., Gibson, D.L., Gonzalez, A., Gorlick, K., Guo, J., Hillmann, B., Holmes, S., Holste, H., Huttenhower, C., Huttley, G.A., Janssen, S., Jarmusch, A.K., Jiang, L., Kaehler, B.D., Kang, K.B., Keefe, C.R., Keim, P., Kelley, S.T., Knights, D., Koester, I., Kosciolek, T., Kreps, J., Langille, M.G.I., Lee, J., Ley, R., Liu, Y.-X., Loftfield, E., Lozupone, C., Maher, M., Marotz, C., Martin, B.D., McDonald, D., McIver, L.J., Melnik, A.V., Metcalf, J.L., Morgan, S.C., Morton, J.T., Naimey, A.T., Navas-Molina, J.A., Nothias, L.F., Orchanian, S.B., Pearson, T., Peoples, S.L., Petras, D., Preuss, M.L., Pruesse, E., Rasmussen, L.B., Rivers, A., Robeson, M.S., Rosenthal, P., Segata, N., Shaffer, M., Shiffer, A., Sinha, R., Song, S.J., Spear, J.R., Swafford, A.D., Thompson, L.R., Torres, P.J., Trinh, P., Tripathi, A., Turnbaugh, P.J., Ul-Hasan, S., van der Hooft, J.J.J., Vargas, F., Vázquez-Baeza, Y., Vogtmann, E., von Hippel, M., Walters, W., Wan, Y., Wang, M., Warren, J., Weber, K. C., Williamson, C.H.D., Willis, A.D., Xu, Z.Z., Zaneveld, J.R., Zhang, Y., Zhu, Q., Knight, R., Caporaso, J.G., 2019. Reproducible, interactive, scalable and extensible microbiome data science using QIIME 2. Nat. Biotechnol. 37, 852–857. https://doi.org/10.1038/s41587-019-0209-9.

Briels, N., Ciesielski, T.M., Herzke, D., Jaspers, V.L.B., 2018. Developmental toxicity of perfluorooctanesulfonate (PFOS) and its chlorinated polyfluoroalkyl ether sulfonate alternative F-53B in the domestic chicken. Environ. Sci. Technol. 52, 12859–12867. https://doi.org/10.1021/acs.est.8b04749.

Cai, Y., Chen, H., Yuan, R., Wang, F., Chen, Z., Zhou, B., 2020. Metagenomic analysis of soil microbial community under PFOA and PFOS stress. Environ. Res. 188, 109838 https://doi.org/10.1016/j.envres.2020.109838.

Carvalhais, L.C., Dennis, P.G., Fedoseyenko, D., Hajirezaei, M.-R., Borriss, R., von Wirén, N., 2011. Root exudation of sugars, amino acids, and organic acids by maize as affected by nitrogen, phosphorus, potassium, and iron deficiency. J. Plant Nutr. Soil Sci. 174, 3–11.

Corrales, I., Poschenrieder, C., Barceló, J., 2008. Boron-induced amelioration of aluminium toxicity in a monocot and a dicot species. J. Plant Physiol. 165, 504–513. https://doi.org/10.1016/j.jplph.2007.03.014.

Deng, M., Wu, Y., Xu, C., Jin, Y., He, X., Wan, J., Yu, X., Rao, H., Tu, W., 2018. Multiple approaches to assess the effects of F-53B, a Chinese PFOS alternative, on thyroid endocrine disruption at environmentally relevant concentrations. Sci. Total Environ. 624, 215–224.

Doornbos, R.F., van Loon, L.C., Bakker, P.A.H.M., 2012. Impact of root exudates and plant defense signaling on bacterial communities in the rhizosphere. A review. Agron. Sustain. Dev. 32, 227–243. https://doi.org/10.1007/s13593-011-0028-y.

Douglas, G.M., Maffei, V.J., Zaneveld, J., Yurgel, S.N., Brown, J.R., Taylor, C.M., Huttenhower, C., Langille, M.G., 2020a. PICRUSt2: an improved and customizable approach for metagenome inference. BioRxiv, 672295.

Douglas, G.M., Maffei, V.J., Zaneveld, J.R., Yurgel, S.N., Brown, J.R., Taylor, C.M., Huttenhower, C., Langille, M.G., 2020b. PICRUSt2 for prediction of metagenome functions. Nat. Biotechnol. 38, 685–688.

Fayle, T.M., Turner, E.C., Foster, W.A., 2013. Ant mosaics occur in SE Asian oil palm plantation but not rain forest and are influenced by the presence of nest-sites and non-native species. Ecography 36, 1051–1057. https://doi.org/10.1111/j.1600-0587.2012.00192.x.

Fierer, N., Lauber, C.L., Ramirez, K.S., Zaneveld, J., Bradford, M.A., Knight, R., 2012. Comparative metagenomic, phylogenetic and physiological analyses of soil microbial communities across nitrogen gradients. ISME J. 6, 1007–1017. https://doi.org/10.1038/ismej.2011.159.

Fisher, R.A., 1936. The use of multiple measurements in taxonomic problems. Ann. Eugen. 7, 179–188.

Fotiadis, D., Kanai, Y., Palacín, M., 2013. The SLC3 and SLC7 families of amino acid transporters. Mol. Aspects Med., The ABCs of membrane transporters in health and disease (SLC series) 34, 139–158. https://doi.org/10.1016/j.mam.2012.10.007.

Galloway, A.F., Akhtar, J., Marcus, S.E., Fletcher, N., Field, K., Knox, P., 2020. Cereal root exudates contain highly structurally complex polysaccharides with soil-binding properties. Plant J. 103, 1666–1678. https://doi.org/10.1111/tpj.14852.

Gao, Y., Deng, S., Du, Z., Liu, K., Yu, G., 2017. Adsorptive removal of emerging polyfluoroalky substances F-53B and PFOS by anion-exchange resin: a comparative study. J. Hazard. Mater. 323, 550–557.

Gomis, M.I., Wang, Z., Scheringer, M., Cousins, I.T., 2015. A modeling assessment of the physicochemical properties and environmental fate of emerging and novel per-and polyfluoroalkyl substances. Sci. Total Environ. 505, 981–991.

Guo, Q., He, Z., Liu, X., Liu, B., Zhang, Y., 2020. High-throughput non-targeted metabolomics study of the effects of perfluorooctane sulfonate (PFOS) on the metabolic characteristics of A. thaliana leaves. Sci. Total Environ. 710, 135542 https://doi.org/10.1016/j.scitotenv.2019.135542.

Gupta, R.S., 2000. The phylogeny of proteobacteria: relationships to other eubacterial phyla and eukaryotes. FEMS Microbiol. Rev. 24, 367–402. https://doi.org/10.1111/j.1574-6976.2000.tb00547.x.

Hale, R., Reich, P., Daniel, T., Lake, P.S., Cavagnaro, T.R., 2018. Assessing changes in structural vegetation and soil properties following riparian restoration. Agric. Ecosyst. Environ. 252, 22–29. https://doi.org/10.1016/j.agee.2017.09.036.

Hu, A., Ju, F., Hou, L., Li, J., Yang, X., Wang, H., Mulla, S.I., Sun, Q., Bürgmann, H., Yu, C.-P., 2017. Strong impact of anthropogenic contamination on the co-occurrence patterns of a riverine microbial community. Environ. Microbiol. 19, 4993–5009. https://doi.org/10.1111/1462-2920.13942.

Hu, L., Robert, C.A.M., Cadot, S., Zhang, X., Ye, M., Li, B., Manzo, D., Chervet, N., Steinger, T., Heijden, M.G.A., van der, Schlaeppi, K., Erb, M., 2018. Root exudate metabolites drive plant-soil feedbacks on growth and defense by shaping the rhizosphere microbiota. Nat. Commun. 9, 1–13. https://doi.org/10.1038/s41467-018-05122-7.

Huang, A.C., Jiang, T., Liu, Y.-X., Bai, Y.-C., Reed, J., Qu, B., Goossens, A., Nützmann, H.-W., Bai, Y., Osbourn, A., 2019. A specialized metabolic network selectively modulates Arabidopsis root microbiota. Science 364, eaau6389. https://doi.org/10.1126/science.aau6389.

Huang, G., Guo, G., Yao, S., Zhang, N., Hu, H., 2016. Organic acids, amino acids compositions in the root exudates and Cu-accumulation in castor (Ricinus communis L.) under Cu stress. Int. J. Phytoremediat. 18, 33–40.

Huang, Q., Chen, Y., Chi, Y., Lin, Y., Zhang, H., Fang, C., Dong, S., 2015. Immunotoxic effects of perfluorooctane sulfonate and di(2-ethylhexyl) phthalate on the marine fish Oryzias melastigma. Fish. Shellfish Immunol. 44, 302–306. https://doi.org/10.1016/j.fsi.2015.02.005.

Huang, S., Millar, A.H., Taylor, N.L., 2011. The plant mitochondrial proteome composition and stress response: conservation and divergence between monocots and dicots. In: Kempken, F. (Ed.), Plant Mitochondria, Advances in Plant Biology. Springer, New York, NY, pp. 207–239. https://doi.org/10.1007/978-0-387-89781-3_9.

Jones, D.L., 1998. Organic acids in the rhizosphere – a critical review. Plant Soil 205, 25–44. https://doi.org/10.1023/A:1004356007312.

Jones, D.L., Farrar, J., Giller, K.E., 2003. Review article associative nitrogen fixation and root exudation-what is theoretically possible in the rhizosphere? Symbiosis.

Kim, M.H., Wang, N., McDonald, T., Chu, K.-H., 2012. Biodefluorination and biotransformation of fluorotelomer alcohols by two alkane-degrading Pseudomonas strains. Biotechnol. Bioeng. 109, 3041–3048. https://doi.org/10.1002/bit.24561.

Kong, Q., Zhang, J., Miao, M., Tian, L., Guo, N., Liang, S., 2013. Partial nitrification and nitrous oxide emission in an intermittently aerated sequencing batch biofilm reactor. Chem. Eng. J. 217, 435–441.

Lakshmanan, V., Selvaraj, G., Bais, H.P., 2014. Functional soil microbiome: belowground solutions to an aboveground problem. Plant Physiol. 166, 689–700. https://doi.org/10.1104/pp.114.245811.

Lechner, M., Knapp, H., 2011. Carryover of perfluorooctanoic acid (PFOA) and perfluorooctane sulfonate (PFOS) from soil to plant and distribution to the different plant compartments studied in cultures of carrots (Daucus carota ssp. Sativus), potatoes (Solanum tuberosum), and cucumbers (Cucumis sativus). J. Agric. Food Chem. 59, 11011–11018. https://doi.org/10.1021/jf201355y.

Li, J., Luo, C., Zhang, D., Cai, X., Jiang, L., Zhao, X., Zhang, G., 2019. Diversity of the active phenanthrene degraders in PAH-polluted soil is shaped by ryegrass rhizosphere and root exudates. Soil Biol. Biochem. 128, 100–110. https://doi.org/10.1016/j.soilbio.2018.10.008.

Li, J., Sun, J., Li, P., 2022. Exposure routes, bioaccumulation and toxic effects of per- and polyfluoroalkyl substances (PFASs) on plants: A critical review. Environ. Int. 158, 106891 https://doi.org/10.1016/j.envint.2021.106891.

Li, M., Rong, L., Zhou, S., Xiao, X., Wu, L., Fan, Y., Lu, C., Zou, X., 2020. Dissipation of sulfonamides in soil emphasizing taxonomy and function of microbiomes by metagenomic analysis. J. Agric. Food Chem. 68, 13594–13607. https://doi.org/10.1021/acs.jafc.0c04496.

Li, P., Sun, J., Xie, X., Li, Z., Huang, B., Zhang, G., Li, J., Xiao, Z., 2021. Stress response and tolerance to perfluorooctane sulfonate (PFOS) in lettuce (Lactuca sativa). J. Hazard. Mater. 404, 124213 https://doi.org/10.1016/j.jhazmat.2020.124213.

Liao, Q., Liu, H., Lu, C., Liu, J., Waigi, M.G., Ling, W., 2021. Root exudates enhance the PAH degradation and degrading gene abundance in soils. Sci. Total Environ. 764, 144436 https://doi.org/10.1016/j.scitotenv.2020.144436.

Liu, P., Cheng, A., Huang, S., Lu, H., Oshida, T., Liu, W., Yu, H., 2020. Body-size scaling is related to gut microbial diversity, metabolism and dietary niche of arboreal folivorous flying squirrels. Sci. Rep. 10, 7809. https://doi.org/10.1038/s41598-020-64801-y.

Liu, W., Li, J., Gao, L., Zhang, Z., Zhao, J., He, X., Zhang, X., 2018. Bioaccumulation and effects of novel chlorinated polyfluorinated ether sulfonate in freshwater alga Scenedesmus obliquus. Environ. Pollut. 233, 8–15. https://doi.org/10.1016/j.envpol.2017.10.039.

Liu, W., Zhao, Q., Zhang, Z., Li, Y., Xu, N., Qu, Q., Lu, T., Pan, X., Qian, H., 2020. Enantioselective effects of imazethapyr on Arabidopsis thaliana root exudates and rhizosphere microbes. Sci. Total Environ. 716, 137121 https://doi.org/10.1016/j.scitotenv.2020.137121.

Louvel, B., Cébron, A., Leyval, C., 2011. Root exudates affect phenanthrene biodegradation, bacterial community and functional gene expression in sand microcosms. Int. Biodeterior. Biodegrad. 65, 947–953. https://doi.org/10.1016/j.ibiod.2011.07.003.

Lu, B., Qian, J., Wang, P., Wang, C., Hu, J., Li, K., He, X., Jin, W., 2020a. Effect of perfluorooctanesulfonate (PFOS) on the rhizosphere soil nitrogen cycling of two riparian plants. Sci. Total Environ. 741, 140494 https://doi.org/10.1016/j.scitotenv.2020.140494.

Lu, B., Qian, J., Wang, P., Wang, C., Hu, J., Li, K., He, X., Jin, W., 2020b. Effect of perfluorooctanesulfonate (PFOS) on the rhizosphere soil nitrogen cycling of two riparian plants. Sci. Total Environ. 741, 140494.

Lu, B., Qian, J., He, F., Wang, P., He, Y., Tang, S., Tian, X., 2022. Effects of long-term perfluorooctane sulfonate (PFOS) exposure on activated sludge performance, composition, and its microbial community. Environ. Pollut. 295, 118684 https://doi.org/10.1016/j.envpol.2021.118684.

Lucini, L., Colla, G., Miras Moreno, M.B., Bernardo, L., Cardarelli, M., Terzi, V., Bonini, P., Rouphael, Y., 2019. Inoculation of Rhizoglomus irregulare or Trichoderma atroviride differentially modulates metabolite profiling of wheat root exudates. Phytochemistry 157, 158–167. https://doi.org/10.1016/j.phytochem.2018.10.033.

Mao, B., Mruk, D., Lian, Q., Ge, R., Li, C., Silvestrini, B., Cheng, C.Y., 2018. Mechanistic insights into PFOS-mediated sertoli cell injury. Trends Mol. Med. 24, 781–793. https://doi.org/10.1016/j.molmed.2018.07.001.

Mapelli, F., Marasco, R., Fusi, M., Scaglia, B., Tsiamis, G., Rolli, E., Fodelianakis, S., Bourtzis, K., Ventura, S., Tambone, F., Adani, F., Borin, S., Daffonchio, D., 2018. The stage of soil development modulates rhizosphere effect along a High Arctic desert chronosequence. ISME J. 1. https://doi.org/10.1038/s41396-017-0026-4.

Meier, I.C., Finzi, A.C., Phillips, R.P., 2017. Root exudates increase N availability by stimulating microbial turnover of fast-cycling N pools. Soil Biol. Biochem. 106, 119–128. https://doi.org/10.1016/j.soilbio.2016.12.004.

Morgan, J.A.W., Bending, G.D., White, P.J., 2005. Biological costs and benefits to plant–microbe interactions in the rhizosphere. J. Exp. Bot. 56, 1729–1739. https://doi.org/10.1093/jxb/eri205.

Nakayama, S., Harada, K., Inoue, K., Sasaki, K., Seery, B., Saito, N., Koizumi, A., 2005. Distributions of perfluorooctanoic acid (PFOA) and perfluorooctane sulfonate (PFOS) in Japan and their toxicities. Environ. Sci. 12, 293–313.

Niederdorfer, R., Fragner, L., Yuan, L., Hausherr, D., Wei, J., Magyar, P., Joss, A., Lehmann, M.F., Ju, F., Bürgmann, H., 2021. Distinct growth stages controlled by the interplay of deterministic and stochastic processes in functional anammox biofilms. Water Res 200, 117225. https://doi.org/10.1016/j.watres.2021.117225.

Pan, M., Chu, L.M., 2016. Adsorption and degradation of five selected antibiotics in agricultural soil. Sci. Total Environ. 545–546, 48–56. https://doi.org/10.1016/j.scitotenv.2015.12.040.

Panchal, P., Miller, A.J., Giri, J., 2021. Organic acids: versatile stress-response roles in plants. J. Exp. Bot. 72, 4038–4052.

Piršelová, B., Kuna, R., Libantová, J., Moravčíková, J., Matušíková, I., 2011. Biochemical and physiological comparison of heavy metal-triggered defense responses in the monocot maize and dicot soybean roots. Mol. Biol. Rep. 38, 3437–3446. https://doi.org/10.1007/s11033-010-0453-z.

Qian, J., Shen, M., Wang, P., Wang, C., Li, K., Liu, J., Lu, B., Tian, X., 2017. Perfluorooctane sulfonate adsorption on powder activated carbon: effect of phosphate (P) competition, pH, and temperature. Chemosphere 182, 215–222. https://doi.org/10.1016/j.chemosphere.2017.05.033.

Qian, J., Lu, B., Chen, Hui, Wang, P., Wang, C., Li, K., Tian, X., Jin, W., He, X., Chen, Hao, 2019. Phytotoxicity and oxidative stress of perfluorooctanesulfonate to two riparian plants: acorus calamus and Phragmites communis. Ecotoxicol. Environ. Saf. 180, 215–226. https://doi.org/10.1016/j.ecoenv.2019.04.078.

Qiao, W., Xie, Z., Zhang, Y., Liu, X., Xie, S., Huang, J., Yu, L., 2018. Perfluoroalkyl substances (PFASs) influence the structure and function of soil bacterial community: greenhouse experiment. Sci. Total Environ. 642, 1118–1126. https://doi.org/10.1016/j.scitotenv.2018.06.113.

Qu, B., Zhao, H., Zhou, J., 2010. Toxic effects of perfluorooctane sulfonate (PFOS) on wheat (Triticum aestivum L.) plant. Chemosphere 79, 555–560. https://doi.org/10.1016/j.chemosphere.2010.02.012.

Rico, C.M., Morales, M.I., McCreary, R., Castillo-Michel, H., Barrios, A.C., Hong, J., Tafoya, A., Lee, W.-Y., Varela-Ramirez, A., Peralta-Videa, J.R., Gardea-Torresdey, J. L., 2013. Cerium oxide nanoparticles modify the antioxidative stress enzyme activities and macromolecule composition in rice seedlings. Environ. Sci. Technol. 47, 14110–14118. https://doi.org/10.1021/es4033887.

Ruan, T., Lin, Y., Wang, T., Liu, R., Jiang, G., 2015. Identification of novel polyfluorinated ether sulfonates as PFOS alternatives in municipal sewage sludge in China. Environ. Sci. Technol. 49, 6519–6527.

Sana, T.R., Fischer, S., Wohlgemuth, G., Katrekar, A., Jung, K., Ronald, P.C., Fiehn, O., 2010. Metabolomic and transcriptomic analysis of the rice response to the bacterial blight pathogen Xanthomonas oryzae pv. oryzae. Metabolomics 6, 451–465. https://doi.org/10.1007/s11306-010-0218-7.

Sheng, S., Chen, F., Li, H., Qian, J., Li, K., Tang, S., Tian, X., 2021. Acute bio-augmentation effect of perfluorooctane sulfonic acid (PFOS) on activated sludge in biological denitrification processes and related stress mechanisms. Environ. Sci. Water Res. Technol. 7, 405–416. https://doi.org/10.1039/D0EW00954G.

Singh, B.K., Millard, P., Whiteley, A.S., Murrell, J.C., 2004. Unravelling rhizosphere–microbial interactions: opportunities and limitations. Trends Microbiol 12, 386–393. https://doi.org/10.1016/j.tim.2004.06.008.

Siqueira, J.O., Nair, M.G., Hammerschmidt, R., Safir, G.R., Putnam, A.R., 1991. Significance of phenolic compounds in plant-soil-microbial systems. Crit. Rev. Plant Sci. 10, 63–121. https://doi.org/10.1080/07352689109382307.

Soda, S., Hamada, T., Yamaoka, Y., Ike, M., Nakazato, H., Saeki, Y., Kasamatsu, T., Sakurai, Y., 2012. Constructed wetlands for advanced treatment of wastewater with a complex matrix from a metal-processing plant: bioconcentration and translocation factors of various metals in Acorus gramineus and Cyperus alternifolius. Ecol. Eng. 39, 63–70. https://doi.org/10.1016/j.ecoleng.2011.11.014.

Stokke, O.S., Thommessen, O.B., 2013. Stockholm convention persistent organic pollutants (Stockholm Convention: POPs). In: Yearbook of International Cooperation on Environment and Development 2001-02. Routledge, pp. 122–123.

Suarez-Fernandez, M., Marhuenda-Egea, F.C., Lopez-Moya, F., Arnao, M.B., Cabrera-Escribano, F., Nueda, M.J., Gunsé, B., Lopez-Llorca, L.V., 2020. Chitosan induces plant hormones and defenses in tomato root exudates. Front. Plant Sci. 11, 1677. https://doi.org/10.3389/fpls.2020.572087.

Sun, C., Zhang, B., Ning, D., Zhang, Y., Dai, T., Wu, L., Li, T., Liu, W., Zhou, J., Wen, X., 2021. Seasonal dynamics of the microbial community in two full-scale wastewater treatment plants: diversity, composition, phylogenetic group based assembly and co-occurrence pattern. Water Res 200, 117295. https://doi.org/10.1016/j.watres.2021.117295.

Sun, Y., Wang, T., Peng, X., Wang, P., Lu, Y., 2016. Bacterial community compositions in sediment polluted by perfluoroalkyl acids (PFAAs) using Illumina high-throughput sequencing. Environ. Sci. Pollut. Res. 23, 10556–10565. https://doi.org/10.1007/s11356-016-6055-0.

Ti, B., Li, L., Liu, J., Chen, C., 2018. Global distribution potential and regional environmental risk of F-53B. Sci. Total Environ. 640–641, 1365–1371. https://doi.org/10.1016/j.scitotenv.2018.05.313.

Tolba, S.R.T., Rosso, L.C., Pentimone, I., Colagiero, M., Moustafa, M.M.A., Elshawaf, I.I. S., Bubici, G., Prigigallo, M.I., Ciancio, A., 2021. Root endophytism by pochonia chlamydosporia affects defense-gene expression in leaves of monocot and dicot hosts under multiple biotic interactions. Plants 10, 718. https://doi.org/10.3390/plants10040718.

Tu, W., Martínez, R., Navarro-Martin, L., Kostyniuk, D.J., Hum, C., Huang, J., Deng, M., Jin, Y., Chan, H.M., Mennigen, J.A., 2019. Bioconcentration and metabolic effects of emerging PFOS alternatives in developing Zebrafish. Environ. Sci. Technol. 53, 13427–13439. https://doi.org/10.1021/acs.est.9b03820.

Tückmantel, T., Leuschner, C., Preusser, S., Kandeler, E., Angst, G., Mueller, C.W., Meier, I.C., 2017. Root exudation patterns in a beech foreSt: Dependence on soil depth, root morphology, and environment. Soil Biol. Biochem. 107, 188–197. https://doi.org/10.1016/j.soilbio.2017.01.006.

Upchurch, R.G., 2008. Fatty acid unsaturation, mobilization, and regulation in the response of plants to stress. Biotechnol. Lett. 30, 967–977. https://doi.org/10.1007/s10529-008-9639-z.

Walker, T.S., Bais, H.P., Grotewold, E., Vivanco, J.M., 2003. Root exudation and rhizosphere biology. Plant Physiol. 132, 44–51. https://doi.org/10.1104/pp.102.019661.

Wang, J., Farooq, T.H., Aslam, A., Shakoor, A., Chen, X., Yan, W., 2021. Non-targeted metabolomics reveal the impact of phenanthrene stress on root exudates of ten urban greening tree species. Environ. Res. 196, 110370 https://doi.org/10.1016/j.envres.2020.110370.

Wang, L., Wang, Li-ao, Zhan, X., Huang, Y., Wang, J., Wang, X., 2020. Response mechanism of microbial community to the environmental stress caused by the different mercury concentration in soils. Ecotoxicol. Environ. Saf. 188, 109906 https://doi.org/10.1016/j.ecoenv.2019.109906.

Wang, S., Huang, J., Yang, Y., Hui, Y., Ge, Y., Larssen, T., Yu, G., Deng, S., Wang, B., Harman, C., 2013. First report of a Chinese PFOS alternative overlooked for 30 years: its toxicity, persistence, and presence in the environment. Environ. Sci. Technol. 47, 10163–10170.

Wang, W., Rhodes, G., Ge, J., Yu, X., Li, H., 2020. Uptake and accumulation of per- and polyfluoroalkyl substances in plants. Chemosphere 261, 127584. https://doi.org/10.1016/j.chemosphere.2020.127584.

Wang, Y., Ren, W., Li, Y., Xu, Y., Teng, Y., Christie, P., Luo, Y., 2019. Nontargeted metabolomic analysis to unravel the impact of di (2-ethylhexyl) phthalate stress on root exudates of alfalfa (Medicago sativa. Sci. Total Environ. 646, 212–219. https://doi.org/10.1016/j.scitotenv.2018.07.247.

de Weert, S., Vermeiren, H., Mulders, I.H.M., Kuiper, I., Hendrickx, N., Bloemberg, G.V., Vanderleyden, J., De Mot, R., Lugtenberg, B.J.J., 2002. Flagella-driven chemotaxis towards exudate components is an important trait for tomato root colonization by pseudomonas fluorescens. Mol. Plan Microbe Interactions® 15, 1173–1180. https://doi.org/10.1094/MPMI.2002.15.11.1173.

Wen, B., Wu, Y., Zhang, H., Liu, Y., Hu, X., Huang, H., Zhang, S., 2016. The roles of protein and lipid in the accumulation and distribution of perfluorooctane sulfonate (PFOS) and perfluorooctanoate (PFOA) in plants grown in biosolids-amended soils. Environ. Pollut. 216, 682–688. https://doi.org/10.1016/j.envpol.2016.06.032.

Wójcik, A., Perczyk, P., Wydro, P., Broniatowski, M., 2018. Effects of water soluble perfluorinated pollutants on phospholipids in model soil decomposer membranes. Biochim. Biophys. Acta BBA Biomembr. 1860, 2576–2587. https://doi.org/10.1016/j.bbamem.2018.09.014.

Wu, H., Wang, X., He, X., Zhang, S., Liang, R., Shen, J., 2017. Effects of root exudates on denitrifier gene abundance, community structure and activity in a micro-polluted constructed wetland. Sci. Total Environ. 598, 697–703. https://doi.org/10.1016/j.scitotenv.2017.04.150.

Zhang, P., Fu, J., Hu, L., 2012. Effects of alkali stress on growth, free amino acids and carbohydrates metabolism in Kentucky bluegrass (Poa pratensis. Ecotoxicology 21, 1911–1918. https://doi.org/10.1007/s10646-012-0924-1.

Zhang, Y., Xie, J.-B., Li, Y., 2017. Effects of increasing root carbon investment on the mortality and resprouting of Haloxylon ammodendron seedlings under drought. Plant Biol. 19, 191–200. https://doi.org/10.1111/plb.12511.

Zhao, H., Guan, Y., Zhang, G., Zhang, Z., Tan, F., Quan, X., Chen, J., 2013. Uptake of perfluorooctane sulfonate (PFOS) by wheat (Triticum aestivum L.) plant. Chemosphere 91, 139–144. https://doi.org/10.1016/j.chemosphere.2012.11.036.

Zhao, L., Huang, Y., Hu, J., Zhou, H., Adeleye, A.S., Keller, A.A., 2016. ^{1}H NMR and GC-MS based metabolomics reveal defense and detoxification mechanism of cucumber plant under nano-Cu stress. Environ. Sci. Technol. 50, 2000–2010. https://doi.org/10.1021/acs.est.5b05011.

Zhu, S., Vivanco, J.M., Manter, D.K., 2016. Nitrogen fertilizer rate affects root exudation, the rhizosphere microbiome and nitrogen-use-efficiency of maize. Appl. Soil Ecol. 107, 324–333.